
Figures and figure supplements

MEGF8 is a modifier of BMP signaling in trigeminal sensory neurons

Caitlin Engelhard, et al.

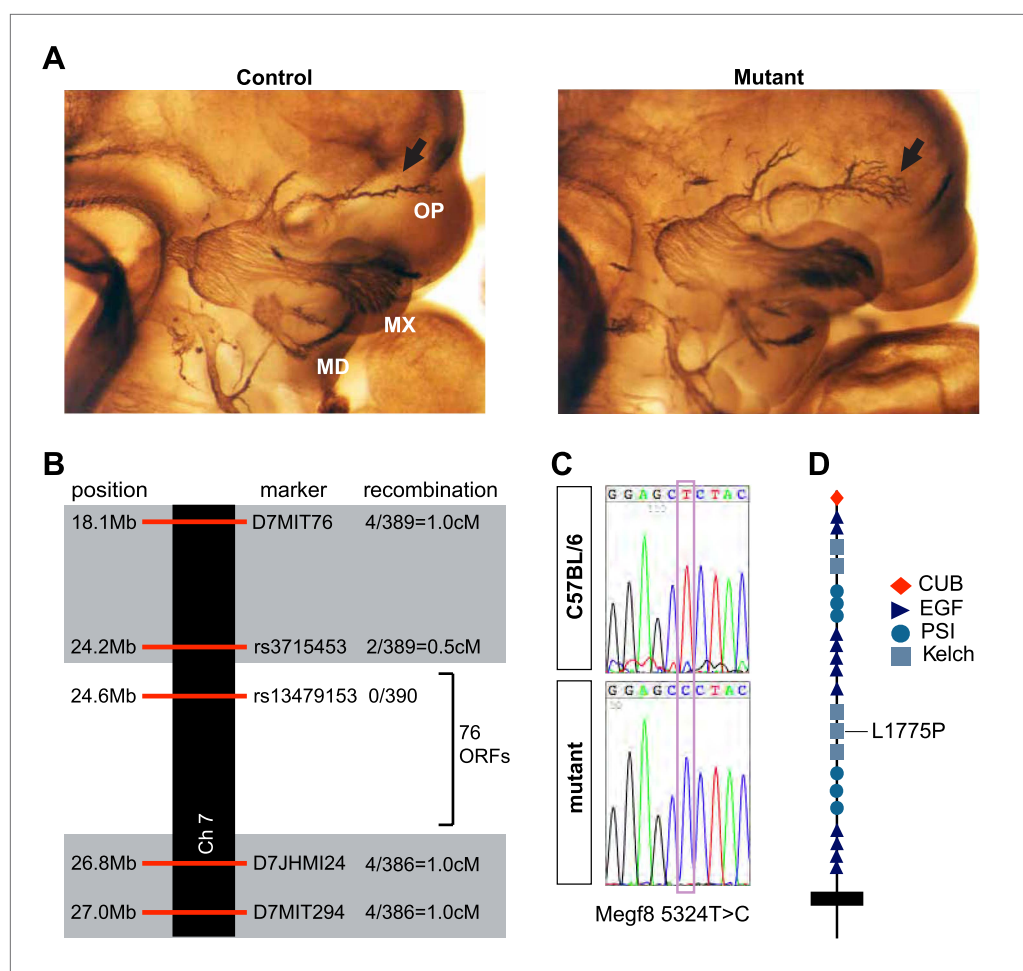


Figure 1. Disruption of *Megf8* causes defasciculation of the TG ophthalmic nerve. **(A)** Whole-mount neurofilament staining of E11.5 control and Line 687 mutant littermates, showing the trigeminal ganglia (TG) and its three main projections: the ophthalmic (OP), maxillary (MX), and mandibular (MD) branches. **(B)** Schematic diagram of the region of Chromosome seven found to contain the Line 687 mutation, the markers used to diagnose linkage, and the frequency of recombination events observed at these markers. ORF, open reading frame. **(C)** Sequence data highlighting the mutation (*Megf8* 5324T>C) observed in Line 687 mutant DNA compared with C57BL/6 wild-type DNA. **(D)** Schematic diagram of *Megf8*. The Line 687 point mutation induces a single amino acid substitution L1775P in a Kelch domain of *Megf8*.

DOI: [10.7554/eLife.01160.003](https://doi.org/10.7554/eLife.01160.003)

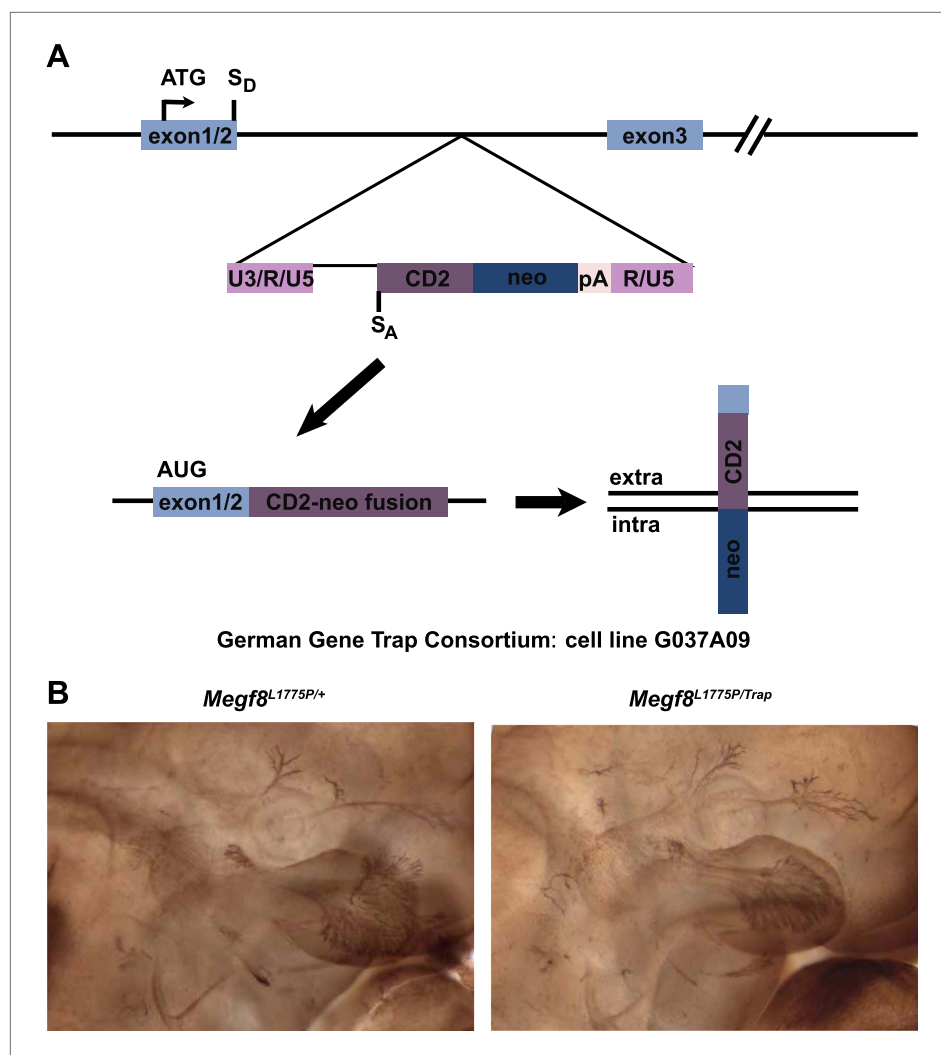


Figure 1—figure supplement 1. Complementation analysis of *Megf8*^{Trap} and *Megf8*^{L1775P} alleles. **(A)** Schematic diagram of gene trap allele (*Megf8*^{Trap}). German Gene Trap Consortium cells G037A09 have an intron 2–3 insertion of a secretory trap vector such that the start ATG and signal peptide of *Megf8* is captured and fused to a CD2-neomycin fusion protein instead of the remaining endogenous locus. S_D = splice donor, S_A = splice acceptor. **(B)** Whole-mount neurofilament staining of E11.5 embryos from an intercross of *Megf8*^{Trap/+} and *Megf8*^{L1775P/+} heterozygotes. Resulting *Megf8*^{L1775P/Trap} embryos have the trigeminal defasciculation phenotype.
DOI: [10.7554/eLife.01160.004](https://doi.org/10.7554/eLife.01160.004)

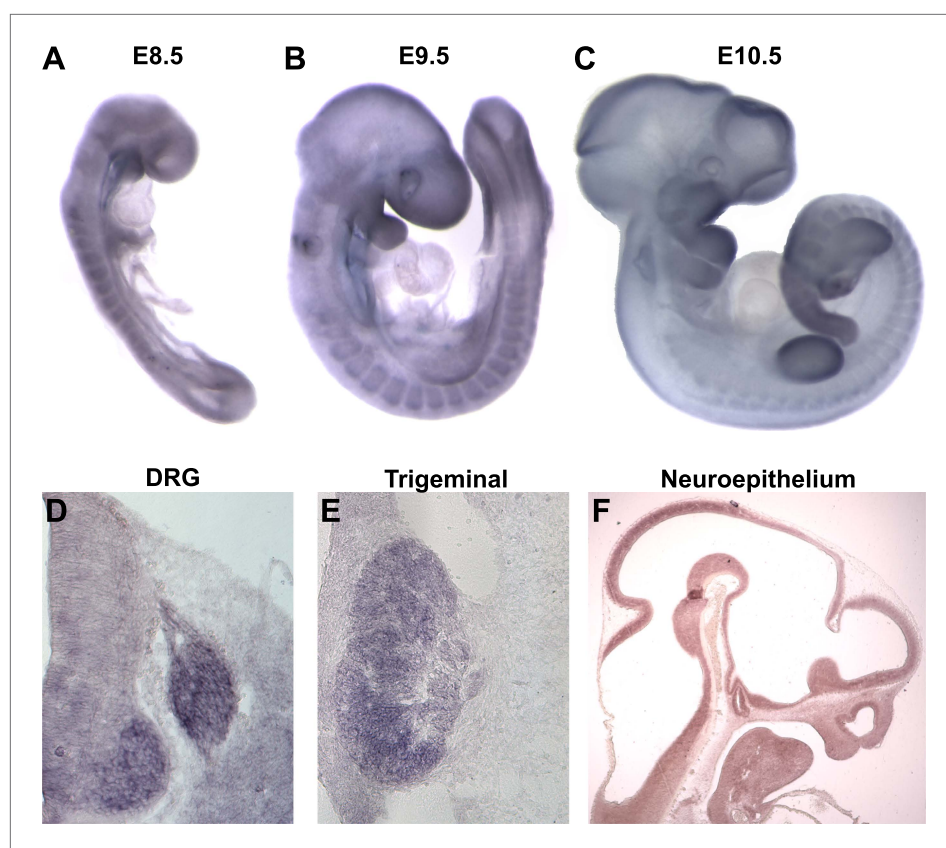


Figure 2. *Megf8* is expressed widely during development. (A–C) Whole-mount in situ hybridization (ISH) for *Megf8* at E8.5, E9.5, and E10.5. (D) ISH for *Megf8* on E11.5 transverse cryosection shows expression in the DRG. (E) ISH for *Megf8* on E11.5 transverse cryosection shows expression in the TG. (F) ISH for *Megf8* on E10.5 paraffin sagittal section shows expression in the developing neuroepithelium.

DOI: [10.7554/eLife.01160.005](https://doi.org/10.7554/eLife.01160.005)

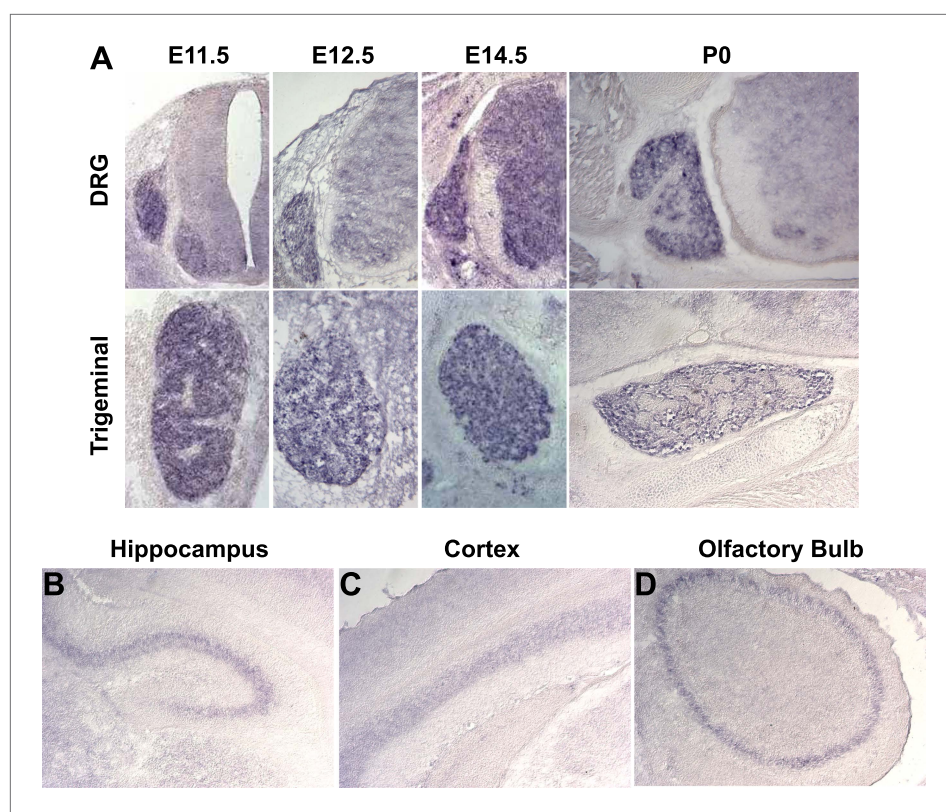


Figure 2—figure supplement 1. *Megf8* is expressed throughout the developing nervous system. (A) In situ hybridization on coronal cryosections from E11.5-P0 shows strong *Megf8* expression at all time points in the DRG and TG. (B–D) In situ hybridization on coronal cryosections at P0 shows strong *Megf8* expression in the hippocampus (B), layer 4/5 of the cortex (C), and in the olfactory bulb (D).

DOI: [10.7554/eLife.01160.006](https://doi.org/10.7554/eLife.01160.006)

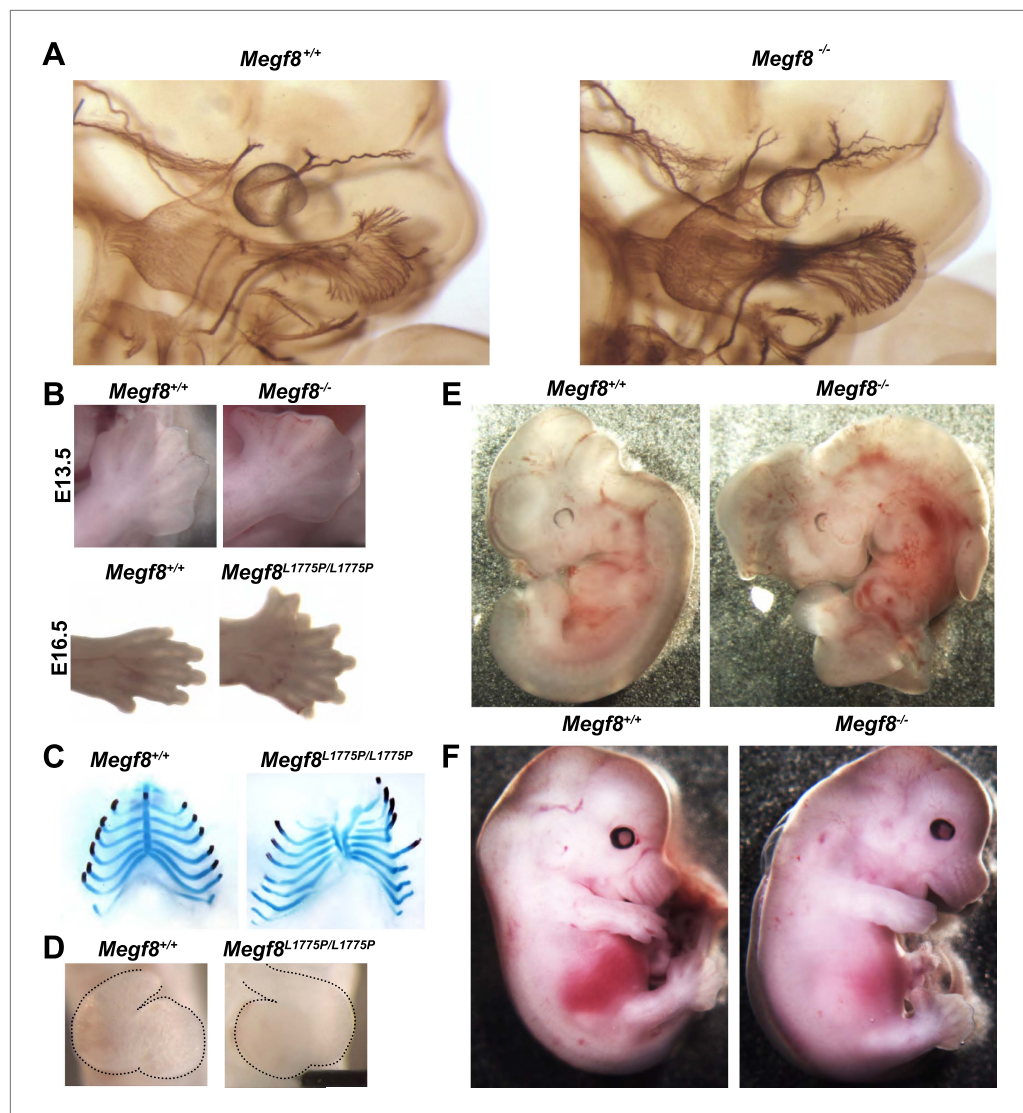


Figure 3. *Megf8* is required for development of the trigeminal ganglia, limb, skeleton, heart, and left-right asymmetry. (A) Whole-mount neurofilament staining of E11.5 *Megf8*^{+/+} and *Megf8*^{-/-} littermates. The *Megf8*^{-/-} null mutant phenocopies the point mutant *Megf8*^{L1775P/L1775P}. (B) Whole-mount images of *Megf8*^{+/+} and *Megf8*^{-/-} hindlimbs at E13.5 (top) and *Megf8*^{+/+} and *Megf8*^{L1775P/L1775P} forelimbs at E16.5 (bottom). (C) Alcian blue and alizarin red staining of E16.5 embryonic ribs/sternum. *Megf8*^{L1775P/L1775P} mutants have a split sternum and delayed ossification of the rib cage. (D) Whole-mount images of the heart of freshly fixed E10.5 embryos with dissected pericardial cavity. *Megf8*^{L1775P/L1775P} have complete left-right inversion of heart looping. Heart is outlined with dotted lines. (E) Whole-mount images of E11.5 *Megf8*^{+/+} and *Megf8*^{-/-} littermates, showing reversal of embryonic turning and exencephaly in the *Megf8*^{-/-}. (F) Whole-mount images of *Megf8*^{+/+} and *Megf8*^{-/-} littermates at E13.5, showing severe edema in the *Megf8*^{-/-}.

DOI: [10.7554/eLife.01160.007](https://doi.org/10.7554/eLife.01160.007)

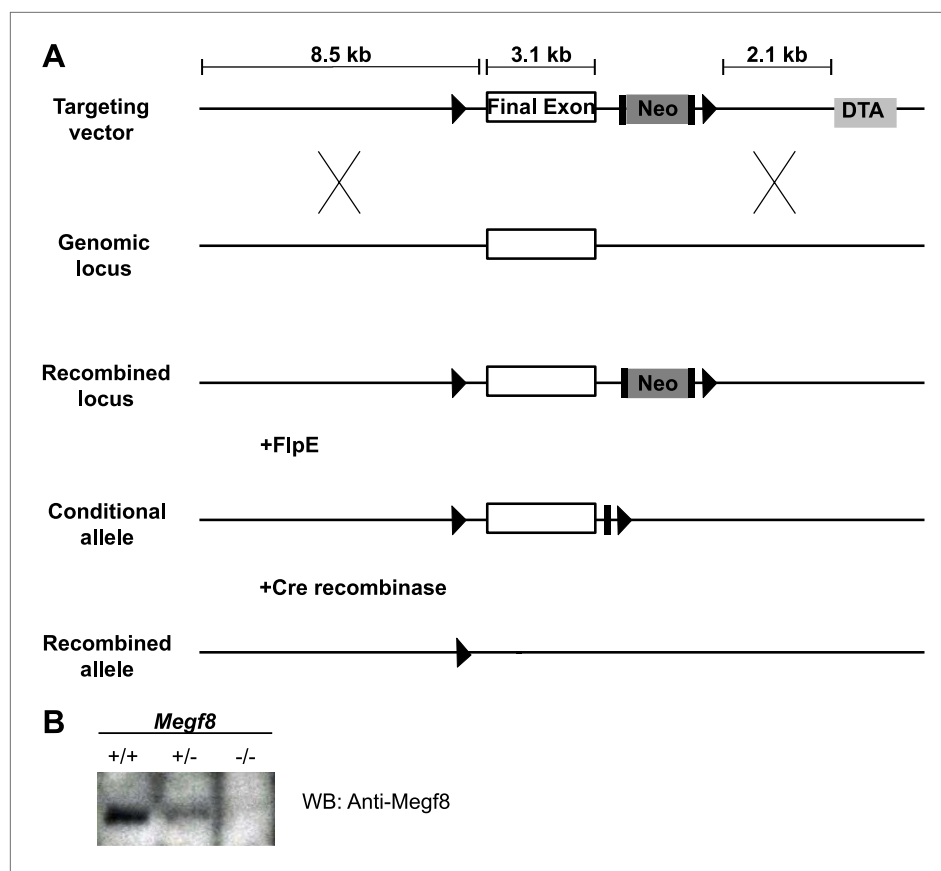


Figure 3—figure supplement 1. Generation of a conditional knock-out mouse line (*Megf8*^{Flox}). **(A)** Schematic diagram of *Megf8* gene targeting strategy. This strategy targeted the final exon of *Megf8*, which is 3.1 kb and comprises the transmembrane domain, intracellular C-terminus, and 3' UTR. A targeting vector was designed with an 8.5 kb long arm, a single loxP site located 500 bp upstream of the targeted exon, a frt-Neo-frt-loxP cassette placed 500 bp downstream of the exon, a 2.1 kb short arm, and a DTA selection cassette. Recombination with the endogenous locus resulted in integration of the 5' loxP and 3' frt-Neo-frt-loxP sites. Following germline transmission, male carriers were then mated with *FlpE* females to excise the neomycin cassette and generate the conditional allele. **(B)** Western blot of E12.5 TG and DRG lysates from *Megf8*^{+/+}, *Megf8*^{+/-}, and *Megf8*^{-/-} littermates. The blot was probed with rabbit anti-Megf8 and shows a loss of Megf8 protein in *Megf8*^{-/-} neurons.

DOI: [10.7554/eLife.01160.008](https://doi.org/10.7554/eLife.01160.008)

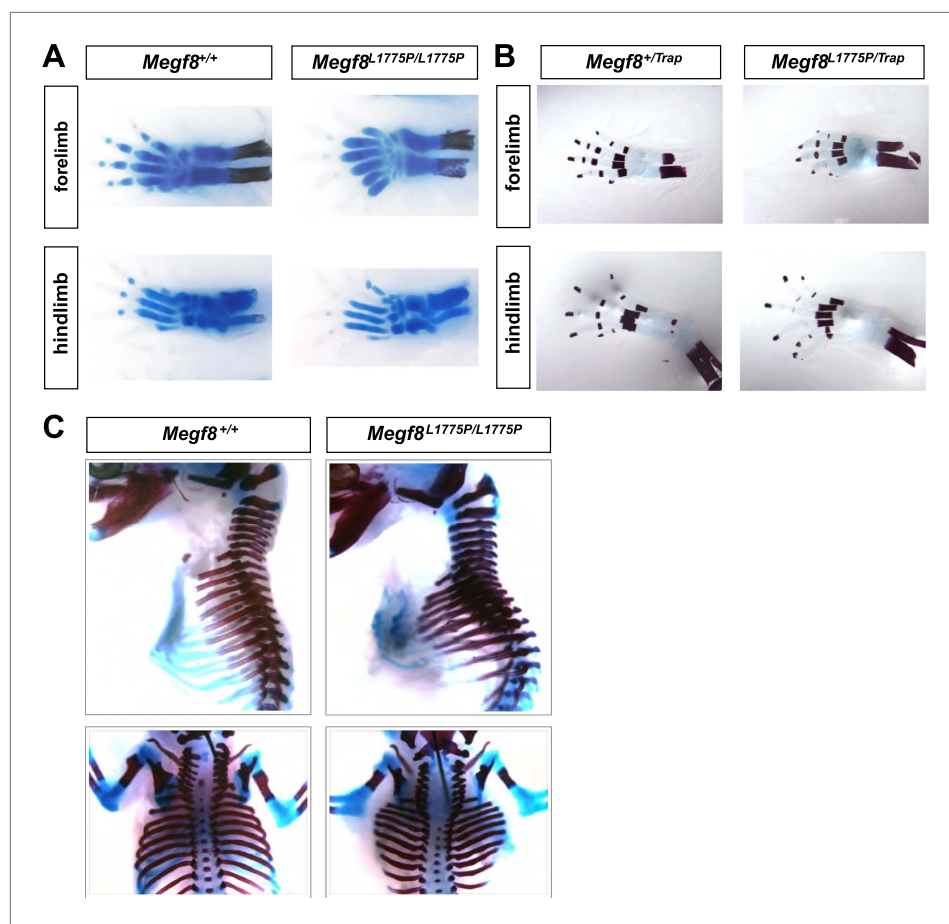


Figure 3—figure supplement 2. *Megf8*^{L1775P/L1775P} mutants show defects in limb and skeletal development. (A) Alcian blue staining on E16.5 limbs shows that *Megf8*^{L1775P/L1775P} mutants have digit duplication as well as duplication of bones in the hand. (B) Alizarin red staining on E16.5 limbs shows that *Megf8*^{L1775P/Trap} mutants have duplication of the bones of the autopodium. (C) Alcian blue and alizarin red staining of whole E16.5 embryos. *Megf8*^{L1775P/L1775P} mutants have a wider and shorter ribcage, delayed ossification of the ribcage, and a split sternum.

DOI: [10.7554/eLife.01160.009](https://doi.org/10.7554/eLife.01160.009)

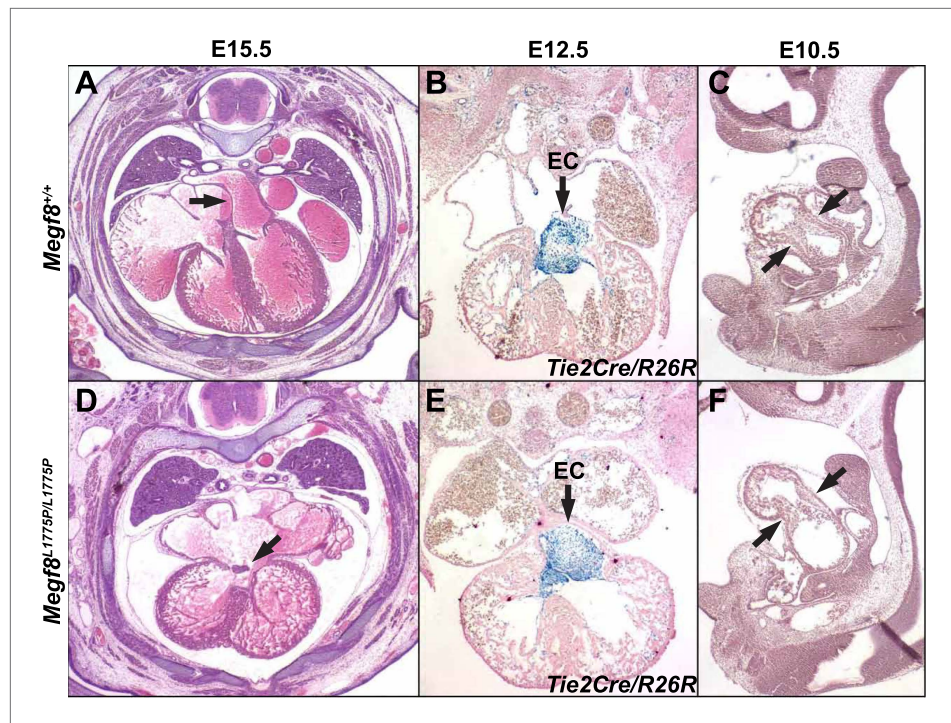


Figure 3—figure supplement 3. Heart development in *Megf8*^{L1775P/L1775P} mutant embryos. Sections from control (A–C) and *Megf8*^{L1775P/L1775P} mutant (D–F) embryos. (A and E) Hematoxylin and eosin (H and E) staining of E15.5 control and mutant sections. The arrowhead in the control E15.5 embryo section points to the atrial septum; the arrowhead in the mutant embryo section points to the vestige of the endocardial cushion, above which the atrial septum is missing and below which the atrioventricular valves are poorly formed or atretic. (B and E) β -galactosidase and nuclear fast red staining of E12.5 embryos, which also carried the *Tie2Cre/R26R* alleles for labeling endothelium and endocardium and derived mesenchymal cells (Kisanuki et al., 2001; Soriano, 1999). Note the normal endocardial cushion (EC) mesenchyme (arrows). (C and F) H and E staining of E10.5 control and mutant sections. Note the apparently normal atrioventricular cushion mesenchyme at E10.5 (arrows).

DOI: [10.7554/eLife.01160.010](https://doi.org/10.7554/eLife.01160.010)

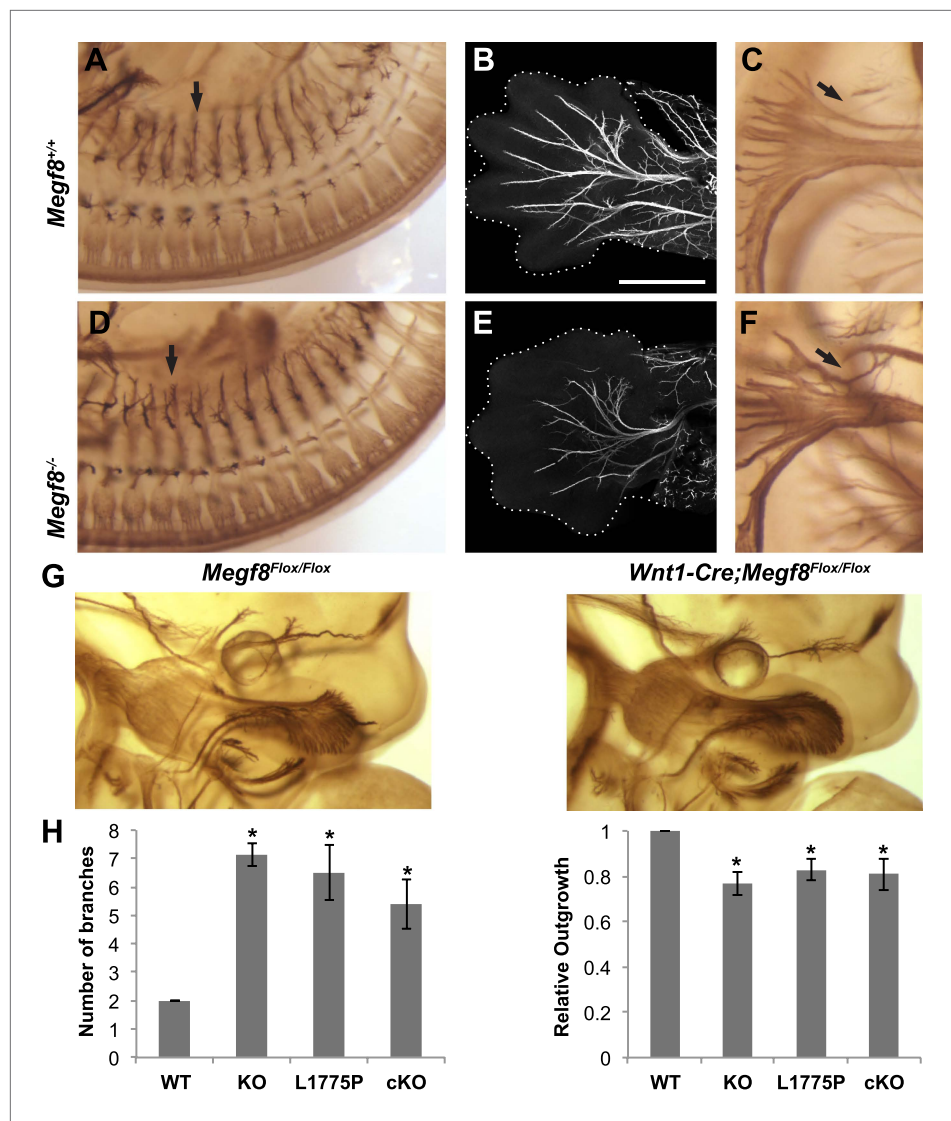


Figure 4. Megf8 is required for development of the PNS. (A and D) Whole-mount neurofilament staining of E11.5 *Megf8*^{+/+} and *Megf8*^{-/-} littermates showing the DRG spinal nerves, which are undergrown in the *Megf8*^{-/-} (arrow). (B and E) Whole-mount peripherin staining of forelimbs from E13.5 *Megf8*^{+/+} and *Megf8*^{-/-} littermates. The radial and ulnar nerves are undergrown in the *Megf8*^{-/-} embryo. Limbs are outlined with dotted lines. Scale bar (B and E) represents 500 μm. (C and F) Whole-mount neurofilament staining of E11.5 *Megf8*^{+/+} and *Megf8*^{-/-} littermates. The vagus/glossopharyngeal nerves are defasciculated in the *Megf8*^{-/-} (arrow). (G) Whole-mount neurofilament staining of E11.5 *Megf8*^{Flox/Flox} and *Wnt1-Cre; Megf8*^{Flox/Flox} littermates. (H) Quantification of ophthalmic branch phenotype for *Megf8*^{-/-} (KO), *Megf8*^{L1775P/L1775P} (L1775P), and *Wnt1-Cre; Megf8*^{Flox/Flox} (cKO) compared to *Megf8*^{+/+} (WT). Left: the number of branches at the nasociliary branch point was significantly greater for KO, L1775P, and cKO embryos. Right: the ophthalmic branch was undergrown in KO, L1775P, and cKO embryos. Four to seven embryos were analyzed per genotype. Error bars represent mean ± s.e.m. *p<0.05, one-way ANOVA. The relative outgrowth was also measured for the maxillary and mandibular branches of the TG for *Megf8*^{-/-} embryos (not shown). The maxillary branch was slightly undergrown compared to *Megf8*^{+/+} (relative outgrowth 0.9, p<0.05) while the mandibular branch was unaffected (relative outgrowth 0.99, p=0.7). To assess defasciculation in the maxillary branch, the relative maxillary area was calculated and no difference was observed between *Megf8*^{+/+} and *Megf8*^{-/-} (relative area 0.94, p=0.2).

DOI: 10.7554/eLife.01160.011

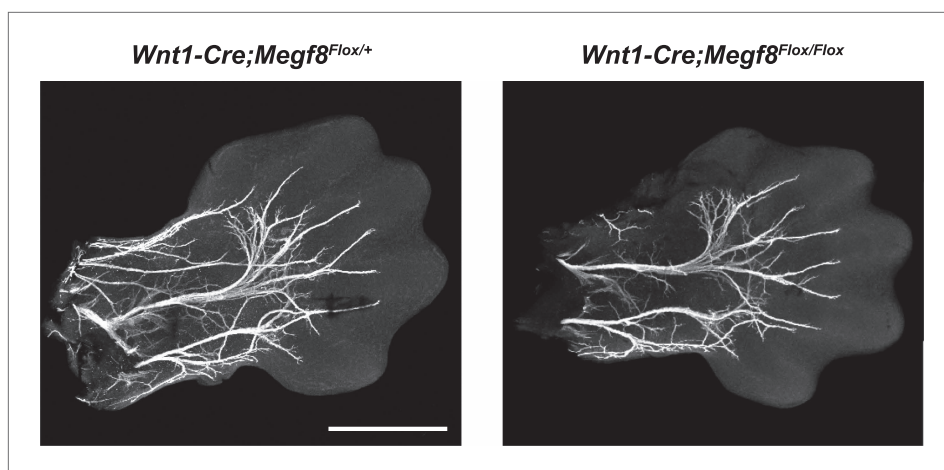


Figure 4—figure supplement 1. Conditional deletion of *Megf8* from DRG neurons does not disrupt formation of the radial/ulnar nerves. Whole-mount peripherin staining of E13.5 forelimbs from *Wnt1-Cre;Megf8^{Flox/+}* and *Wnt1-Cre;Megf8^{Flox/Flox}* littermates. Limbs are outlined with dotted lines. Scale bar represents 500 μ m.
DOI: [10.7554/eLife.01160.012](https://doi.org/10.7554/eLife.01160.012)

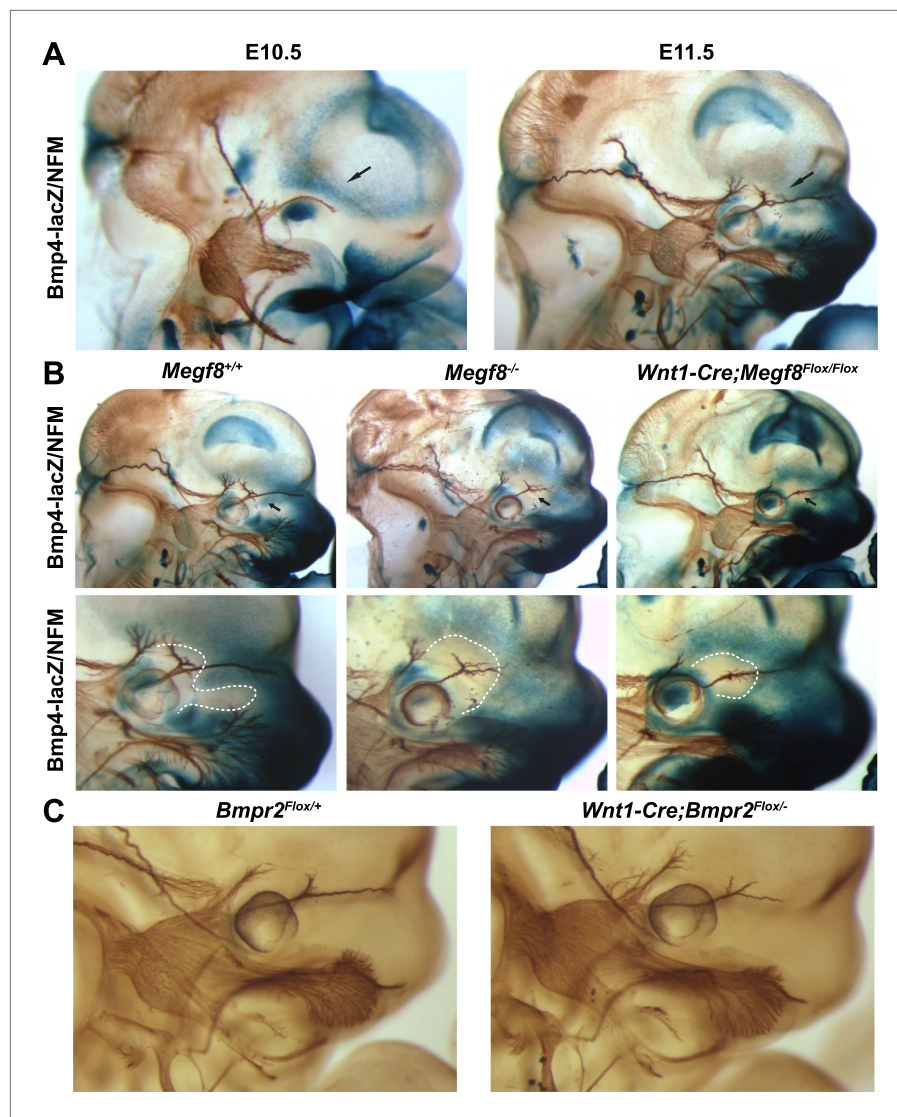


Figure 5. BMP signaling is required for proper extension of the TG ophthalmic nerve. (A) Whole-mount β -galactosidase and neurofilament (NFM) co-staining on *Bmp4*^{lacZ/+} embryos at E10.5 and E11.5, showing the relationship between *Bmp4* expression and the developing TG nerve. (B) Whole-mount β -galactosidase and neurofilament co-staining on E11.5 embryos: *Bmp4*^{lacZ/+}; *Megf8*^{+/+} (left) and *Bmp4*^{lacZ/+}; *Megf8*^{-/-} (center) littermates, as well as *Bmp4*^{lacZ/+}; *Wnt1-Cre*; *Megf8*^{Flox/Flox} (right). *Bmp4*^{lacZ} expression is lost at the location where defasciculation of the TG ophthalmic nerve occurs in *Megf8*^{-/-} and *Wnt1-Cre*; *Megf8*^{Flox/Flox} embryos. The top row shows the whole head with all three TG branches. The bottom row is an enlargement of the top row showing the ophthalmic branch. The area of perturbed *Bmp4* expression is outlined. The disruption of *Bmp4*^{lacZ} expression was fully penetrant and observed in all *Megf8*^{-/-} (n = 4) and *Wnt1-Cre*; *Megf8*^{Flox/Flox} (n = 3) embryos assessed. (C) Whole-mount neurofilament staining of E11.5 *Bmpr2*^{Flox/+} and *Wnt1-Cre*; *Bmpr2*^{Flox/-} littermates.

DOI: [10.7554/eLife.01160.014](https://doi.org/10.7554/eLife.01160.014)

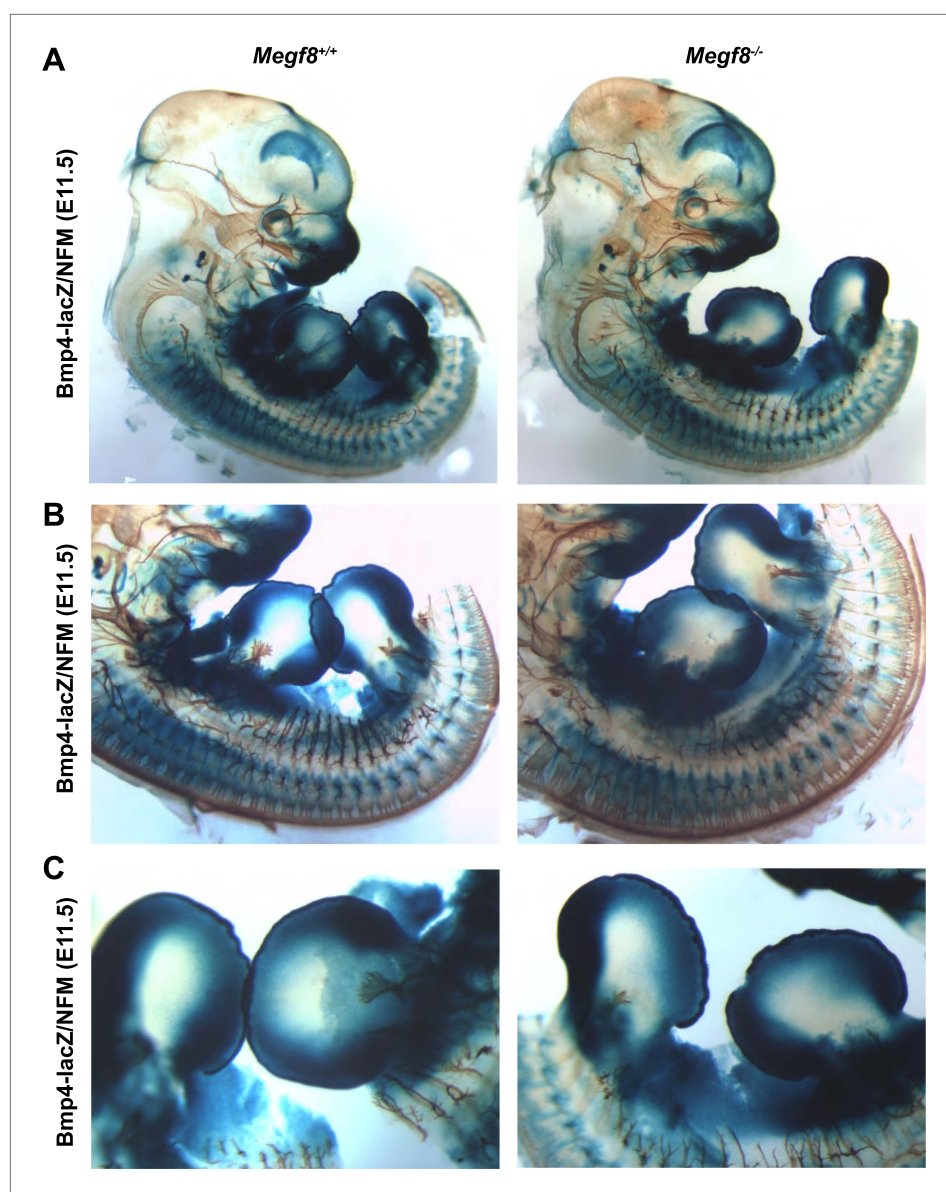


Figure 5—figure supplement 1. *Bmp4* expression in *Megf8*^{-/-} embryo compared to wild-type littermate. Whole-mount β-galactosidase and neurofilament co-staining on E11.5 embryos: *Bmp4*^{lacZ/+};*Megf8*^{+/+} (left) and *Bmp4*^{lacZ/+};*Megf8*^{-/-} (right) littermates. *Bmp4*^{lacZ} expression is lost at the location where defasciculation of the TG ophthalmic nerve occurs in *Megf8*^{-/-} embryos but is intact throughout the rest of the embryo. (A) Presentation of the whole embryo. (B) DRG and spinal nerves. (C) Forelimbs and hindlimbs.

DOI: [10.7554/eLife.01160.015](https://doi.org/10.7554/eLife.01160.015)

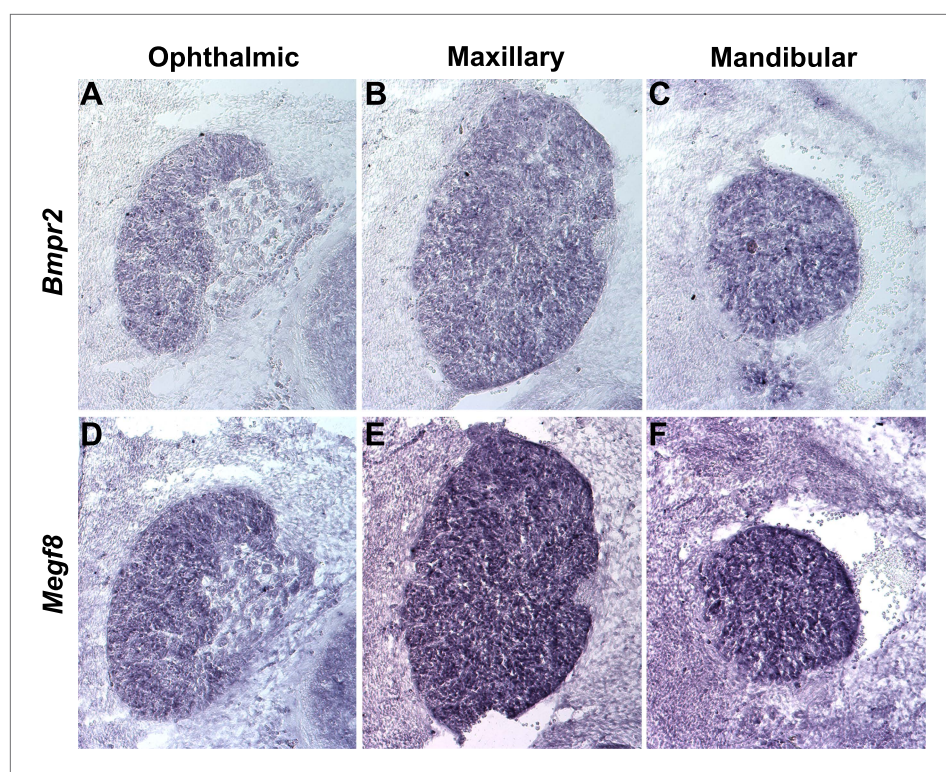


Figure 5—figure supplement 2. *Bmpr2* and *Megf8* are expressed throughout the developing TG. In situ hybridization on serial transverse cryosections at E12.5 shows strong expression of *Bmpr2* (A–C) and *Megf8* (D–F) throughout the developing TG. Representative images are shown for ophthalmic (A and D), maxillary (B and E), and mandibular (C and F) lobes of the TG.

DOI: [10.7554/eLife.01160.016](https://doi.org/10.7554/eLife.01160.016)

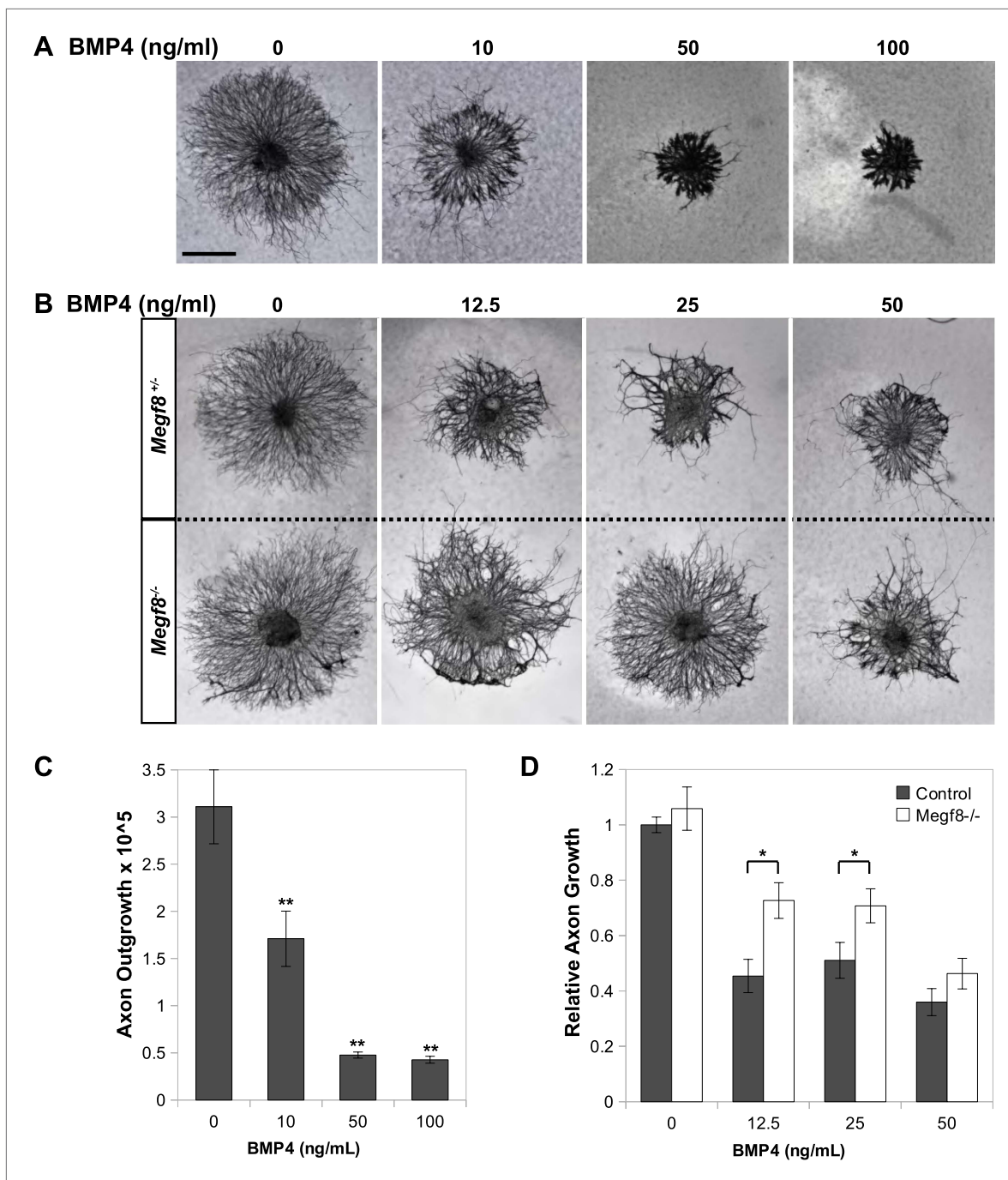


Figure 6. Megf8 mediates the inhibition of TG axon growth by BMP4. **(A)** E12.5 wild-type TG explants cultured in 0–100 ng/ml BMP4. **(B)** E12.5 TG explants from *Megf8*^{+/-} and *Megf8*^{-/-} littermates cultured side by side in 0–50 ng/ml BMP4. **(C)** Quantification of **(A)**: axonal outgrowth of wild-type TG explants in the presence of 0–100 ng/ml BMP4. Increasing doses of BMP4 caused robust inhibition of axon outgrowth (** $p < 0.05$, Student's *t* test). Three to four explants were quantified for each concentration of BMP4. Error bars represent mean \pm SEM. **(D)** Quantification of **(B)**: relative axon outgrowth of TG explants from control (*Megf8*^{+/-} or *Megf8*^{-/-}) and *Megf8*^{-/-} littermates in the presence of 0–50 ng/ml BMP4. BMP4 inhibition of axon outgrowth is partially lost in *Megf8*^{-/-} explants (* $p < 0.05$, Student's *t* test). The experiment was repeated three times, using three to four explants per BMP4 concentration in each experiment; each bar represents results from at least 10 explants. Error bars represent mean \pm SEM. Scale bar represents 20 μ m.

DOI: [10.7554/eLife.01160.017](https://doi.org/10.7554/eLife.01160.017)